

Supporting Information

A Series of Oxsulfides $\text{RE}_2\text{M}_2\text{S}_3\text{O}_4$ ($\text{RE} = \text{Y, Tm}$; $\text{M} = \text{Zr, Hf}$) Featuring Unique MS_3O_4 Motif and $[\text{M}_2\text{S}_3\text{O}_4]^{8-}$ Wrinkle Layer

Zhen-Tao Lu, Si-Han Yang, Wenlong Liu* and Sheng-Ping Guo*

School of Chemistry and Chemical Engineering, Yangzhou University, Yangzhou, Jiangsu 225002, P. R. China

Experimental Section

Synthesis. High-temperature solid-state method was taken to synthesize the crystals of $\text{Y}_2\text{Zr}_2\text{S}_3\text{O}_4$ (**1**), $\text{Y}_2\text{Hf}_2\text{S}_3\text{O}_4$ (**2**), and $\text{Tm}_2\text{Zr}_2\text{S}_3\text{O}_4$ (**3**). The commercial regents $\text{Y}_2\text{O}_3/\text{Tm}_2\text{O}_3$ (99.99 %, Aladdin), $\text{ZrO}_2/\text{HfO}_2$ (99.9 %, Aladdin), B (99 %, Aladdin), and S (99.9 %, Aladdin) were used with the molar ratios of 1 : 1 : 4 : 5, and the total mixture was 500 mg. Additional 400 mg KI (99 %, Aladdin) was added as the flux. For a typical reaction, the mixture was ground into fine powder, then pressed into a pellet, which was then flame-sealed into a quartz tube under 1×10^{-4} torr. The quartz tube was put in a muffle furnace and heated to 950 °C in 25 h and kept for 7 days, and then cooled down to 300 °C in 5 days. The transparent rod-like crystals with low yields were obtained.

Structure Refinement and Crystal Data. The single crystal data of **1–3** were collected via a Bruker D8 QUEST X-ray diffractometer with graphite-monochromated Mo-K α radiation ($\lambda = 0.71073 \text{ \AA}$). The SHELXTL program package was used to determine the crystal structures. The crystal structures were solved based on Direct Method, and full-matrix least-squares technique on F^2 with anisotropic displacement parameters for all atoms was used to refine the data. A secondary extinction correction was included by the final refinement. Table S1, S2, and S3 list the refinement and crystallographic data, thermal parameters and atomic coordinates, and selected bond lengths, respectively.

Power X-ray Diffraction (PXRD) Characterization. A Bruker D8 Advanced powder X-ray diffractometer was used to measure the PXRD patterns for **1–3** at room temperature. The scan parameters were set at 40 kV and 40 mA for Cu-K α radiation ($\lambda = 1.5406 \text{ \AA}$) and the scan speed was 5°/min.

UV-vis-NIR Diffuse Reflectance Spectroscopy. A Carry 5000 UV-vis-NIR Absorption Spectrometer with an integrating sphere attachment was used to record the diffuse reflectance spectra for the powder crystalline samples of **1–3**.

Magnetic susceptibility measurement. Temperature-dependent magnetic susceptibility of **3** was measured by a Quantum Design PPMS from 2 to 300 K in an applied magnetic field of 1000 Oe. The polycrystalline powdery sample was secured in a gel capsule. The diamagnetic correction was made using Pascal's constants.

Theoretical calculation. The CASTEP module in Material Studio,⁴ which is based on density functional theory (DFT), was used to build the calculation model. Their band structure, density of states (DOS), and optical properties were calculated. The plane-wave cut-off energies were set at 380 eV for **1** and **2** within ultrasoft pseudopotential. Monkhorst-Pack k-points meshes were all $4 \times 2 \times 7$ for them, and the threshold was set at 5×10^{-7} eV. The electrons on Y-4d¹5s², Zr-4d²5s², S-3s²3p⁴, and O-2s²2p⁴ for **1**, and Y-4d¹5s², Hf-5d²6s², S-3s²3p⁴, and O-2s²2p⁴ for **2** were selected as valence electrons. The Fermi level at 0 eV was chosen as the reference.

The optical properties described in terms of the complex dielectric function $\epsilon(\omega) = \epsilon_1(\omega) + i\epsilon_2(\omega)$ were calculated. $\epsilon_1(\omega)$ and $i\epsilon_2(\omega)$ represent the real and imaginary parts of dielectric function, respectively.^{5,6} $\epsilon_2(\omega)$ can be used to generate other optical constants using the Kramers-Kroning transform.^{7,8} The first-order nonresonant susceptibility at the low-frequency region is given by $\chi^{(1)}(\omega) = \epsilon_1(\omega) - 1$. Refractive index n was obtained using the below equation,

$$n(\omega) = \sqrt{\frac{\epsilon_1^2(\omega) + \epsilon_2^2(\omega) + \epsilon_1(\omega)}{2}} \quad (1)$$

Table S1. Crystal data and structure refinement parameters for **1**, **2**, and **3**.

chemical formula	1	2	3
Fw	520.44	694.98	680.48
T (K)		298	
crystal system, space group		orthorhombic, <i>Pbam</i>	
<i>Z</i>		2	
<i>a</i> (Å)	6.5120(8)	6.5013(8)	6.4784 (7)
<i>b</i> (Å)	14.185(2)	14.1770(15)	14.1361 (16)
<i>c</i> (Å)	3.6772(5)	3.6710(4)	3.6618 (5)
<i>V</i> (Å ³)	339.68(8)	338.35(7)	335.35 (7)
<i>D</i> _{calcd} (g cm ⁻³)	5.088	6.822	6.739
μ (mm ⁻¹)	20.765	48.426	30.098
<i>F</i> (000)	476	604	596
2θ range (°)	5.744 to 54.856	5.748 to 49.88	5.764 to 53
measd. reflns	2682	2093	1307
indep. reflns/R _{int}	452/0.0376	342/0.0410	402/0.0304
obs. reflns	398	336	357
R1, wR2 (<i>I</i> > 2σ(<i>I</i>)) ^a	0.0226, 0.0474	0.0276, 0.0737	0.0306, 0.0723
R1, wR2(all data) ^a	0.0290, 0.0491	0.0281, 0.0743	0.0353, 0.0742
GOF on <i>F</i> ²	1.038	1.046	1.048
Δρ _{max} /Δρ _{min} , e/Å ³	0.89/-0.91	2.00/-1.95	2.10/-1.97

^aR1 = ||*F*_o - |*F*_c||/|*F*_o|; wR2 = [*w*(*F*_o² - *F*_c²)²]/[*w*(*F*_o²)²]^{1/2}.

Table S2. Atomic coordinates ($\times 10^4$) and equivalent isotropic displacement parameters (U_{eq}^a , $\text{\AA}^2 \times 10^3$) for **1**, **2**, and **3**.

atom	x	y	z	$U_{\text{eq}}/\text{\AA}^2$
1				
Y(1)	7147.4(9)	6617.1(4)	0	6.9(2)
Zr(1)	2928.7(9)	5727.6(4)	5000	4.3(2)
S(1)	0	5000	0	8.5(4)
S(2)	244(2)	7119.5(11)	5000	8.0(3)
O(1)	3639(6)	4310(3)	5000	6.1(9)
O(2)	3758(6)	6220(3)	0	9.9(9)
2				
Y(1)	7148.0(16)	6616.7 (8)	0	2.0(4)
Hf(1)	2939.6(7)	5724.1(3)	5000	3.4(3)
S(1)	0	5000	0	8.1(9)
S(2)	276(4)	7111.6(19)	5000	5.0 (6)
O(1)	3668(14)	4319(5)	5000	3.6(18)
O(2)	3774(13)	6227(5)	0	6.0(17)
3				
Tm(1)	7132.9(9)	6619.5(5)	0	6.7(2)
Zr(1)	2915.1(19)	5728.2(9)	5000	0.8(3)
S(1)	0	5000	0	7.3(10)
S(2)	209(5)	7121(3)	5000	6.1(7)
O(1)	3639(16)	4301(6)	5000	6.2(19)
O(2)	37421(17)	6215(7)	0	11(2)

^a U_{eq} is defined as one third of the trace of the orthogonalized U_{ij} tensor.

Table S3. Important bond lengths (\AA) for **1**, **2**, and **3**.

Bond	Dist./ \AA	Bond	Dist./ \AA
1			
Zr(1)–S(1)	2.843(1)	Y(1)–S(1)#6	2.952(1)
Zr(1)–S(2)	2.637(2)	Y(1)–S(2)#6	2.820(1)
Zr(1)–O(1)	2.063(4)	Y(1)–S(2)#7	2.851(1)
Zr(1)–O(1)#5	2.236(4)	Y(1)–O(1)#5	2.318(2)
Zr(1)–O(2)	2.040(2)	Y(1)–O(2)	2.278(4)
2			
Hf(1)–S(1)	2.842(1)	Y(1)–S(1)#6	2.948(1)
Hf(1)–S(2)	2.621(3)	Y(1)–S(2)#6	2.828(2)
Hf(1)–O(1)	2.047(7)	Y(1)–S(2)#7	2.846(2)
Hf(1)–O(1)#1	2.207(9)	Y(1)–O(1)#1	2.326(4)
Hf(1)–O(2)	2.042(3)	Y(1)–O(2)	2.262(8)
3			
Tm(1)–S(1)#6	2.948(1)	Zr(1)–S(1)	2.825(1)
Tm(1)–S(2)#6	2.798(3)	Zr(1)–S(2)	2.636(4)
Tm(1)–S(2)#7	2.842(3)	Zr(1)–O(1)	2.071(9)
Tm(1)–O(1)#2	2.301(6)	Zr(1)–O(1)#2	2.233(10)
Tm(1)–O(2)	2.271(11)	Zr(1)–O(2)	2.028(4)

Symmetry transformations used to generate equivalent atoms: #1 $+x, +y, 1-z$; #2 $+x, +y, -z$; #3 $+x, +y, -1+z$; #4 $+x, +y, 1+z$; #5 $1-x, 1-y, 1-z$; #6 $1+x, +y, +z$; #7 $1/2+x, 3/2-y, +z$; #8 $1+x, +y, -1+z$; #9 $1/2+x, 3/2-y, -1+z$; #10 $1-x, 1-y, -z$; #11 $1-x, 1-y, -z$; #12 $-1+x, +y, z$; #13 $-1/2+x, 3/2-y, +z$; #14 $-1+x, +y, 1+z$; #15 $-1/2+x, 3/2-y, 1+z$ for **1**. #1 $1-x, 1-y, 1-z$; #2 $1-x, 1-y, -z$; #3 $+x, +y, 1+z$; #4 $+x, +y, -1+z$; #5 $+x, +y, 1-z$; #6 $1+x, +y, z$; #7 $1/2+x, 3/2-y, -1+z$; #8 $1/2+x, 3/2-y, +z$; #9 $1+x, y, -1+z$; #10 $-x, 1-y, 1-z$; #11 $-x, 1-y, -z$; #12 $-1+x, y, z$; #13 $-1/2+x, 3/2-y, +z$; #14 $-1+x, +y, 1+z$; #15 $-1/2+x, 3/2-y, 1+z$ for **2**. #1 $+x, +y, 1-z$; #2 $1-x, 1-y, 1-z$; #3 $+x, +y, -1+z$; #4 $+x, +y, 1+z$; #5 $1-x, 1-y, -z$; #6 $1+x, +y, +z$; #7 $1/2+x, 3/2-y, -1+z$; #8 $1+x, +y, -1+z$; #9 $1/2+x, 3/2-y, +z$; #10 $+x, +y, -z$; #11 $-x, 1-y, 1-z$; #12 $-x, 1-y, -z$; #13 $-1+x, +y, +z$; #14 $-1/2+x, +y, 1+z$; #15 $-1+x, +y, 1+z$; #16 $-1/2+x, 3/2-y, 1+z$ for **3**.

Table S4. Known *RE*–Ti/Zr/Hf–O–S oxysulfides.

Compound	Crystal System	Space Group	Reference
Ce ₂₀ Ti ₁₁ S ₄₄ O ₆	Orthorhombic	<i>Pmmn</i>	9
La ₂₀ Ti ₁₁ S ₄₄ O ₆	Orthorhombic	<i>Pmmn</i>	10
La ₄ Ti ₃ S ₄ O ₈	Monoclinic	<i>C2/m</i>	11
La ₆ Ti ₂ S ₈ O ₅	Monoclinic	<i>P2₁/m</i>	11
La ₈ Ti ₁₀ S ₂₄ O ₄	Tetragonal	<i>P4/mmm</i>	12
Nd ₁₆ Ti ₅ S ₁₇ O ₁₇	Tetragonal	<i>I4/m</i>	13
Nd ₂ Ti ₂ S ₂ O ₅	Tetragonal	<i>I4/mmm</i>	14
Pr ₂ Ti ₂ S ₂ O ₅	Tetragonal	<i>I4/mmm</i>	14
Sm ₂ Ti ₂ S ₂ O ₅	Tetragonal	<i>I4/mmm</i>	14
Gd ₂ Ti ₂ S ₂ O ₅	Tetragonal	<i>I4/mmm</i>	14
Tb ₂ Ti ₂ S ₂ O ₅	Tetragonal	<i>I4/mmm</i>	14
Dy ₂ Ti ₂ S ₂ O ₅	Tetragonal	<i>I4/mmm</i>	14
Ho ₂ Ti ₂ S ₂ O ₅	Tetragonal	<i>I4/mmm</i>	14
Er ₂ Ti ₂ S ₂ O ₅	Tetragonal	<i>I4/mmm</i>	14
Y ₂ Ti ₂ S ₂ O ₅	Tetragonal	<i>I4/mmm</i>	14
Pr ₆ Ti ₂ S ₇ O ₆	Monoclinic	<i>P2₁/m</i>	15

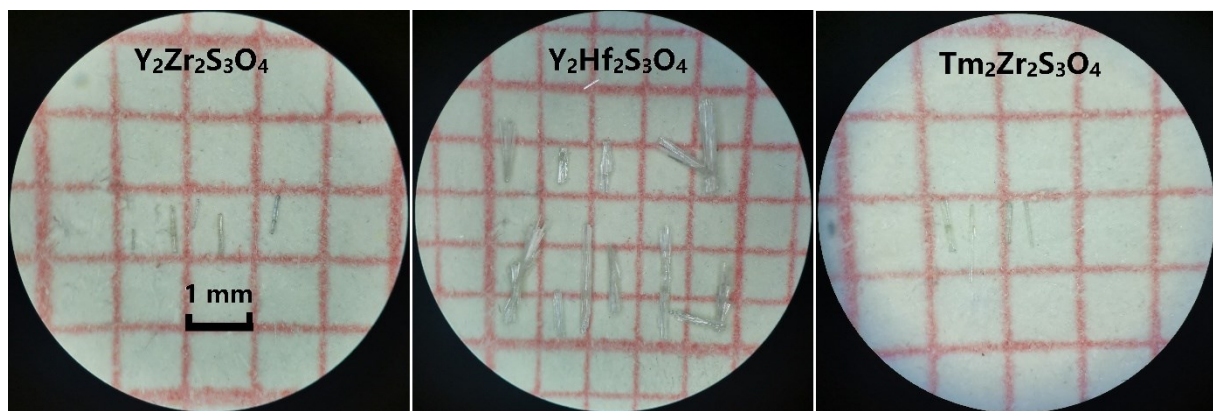


Fig. S1 Photos for the crystals of **1–3**.

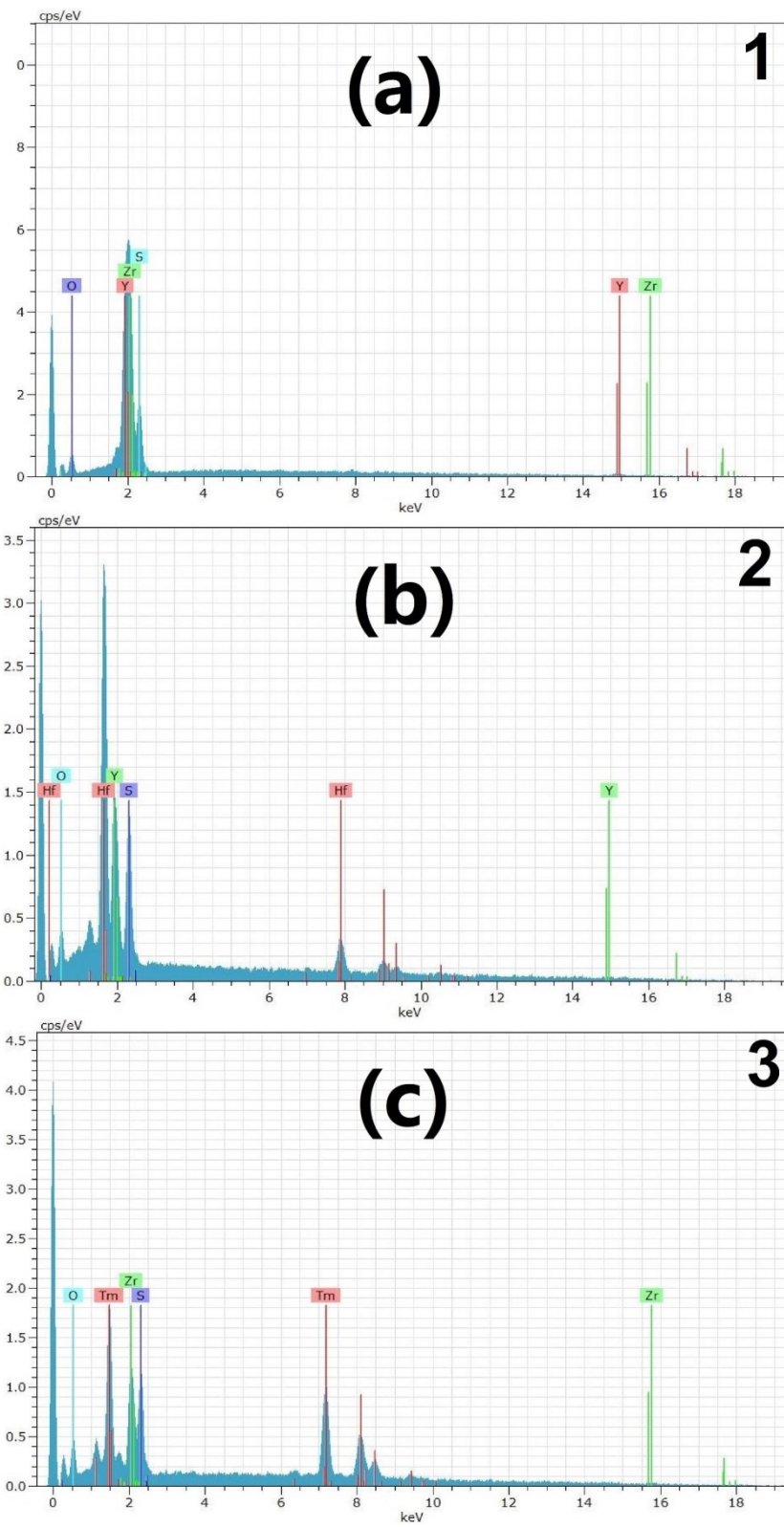


Fig. S2 EDS images for **1** (a), **2** (b), and **3** (c).

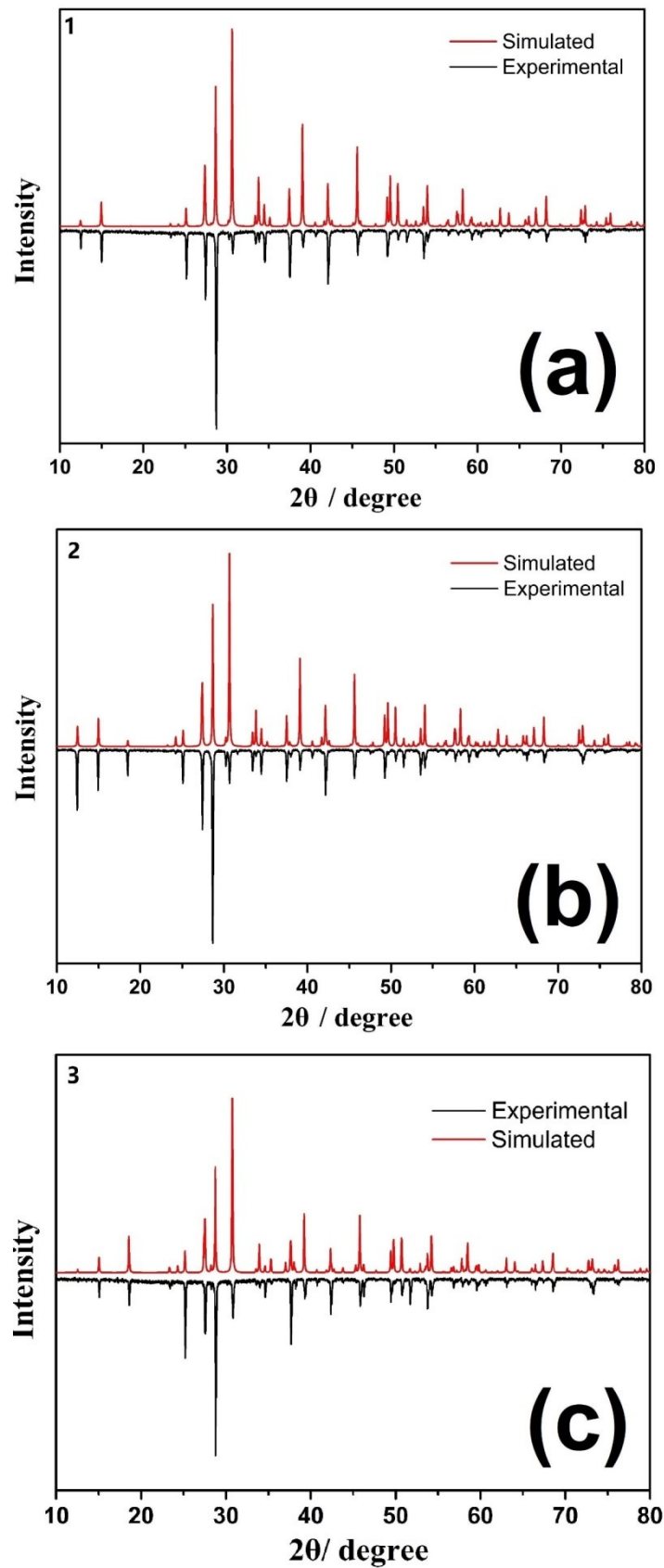


Fig. S3 Powder X-ray diffraction patterns for **1** (a), **2** (b), and **3** (c).

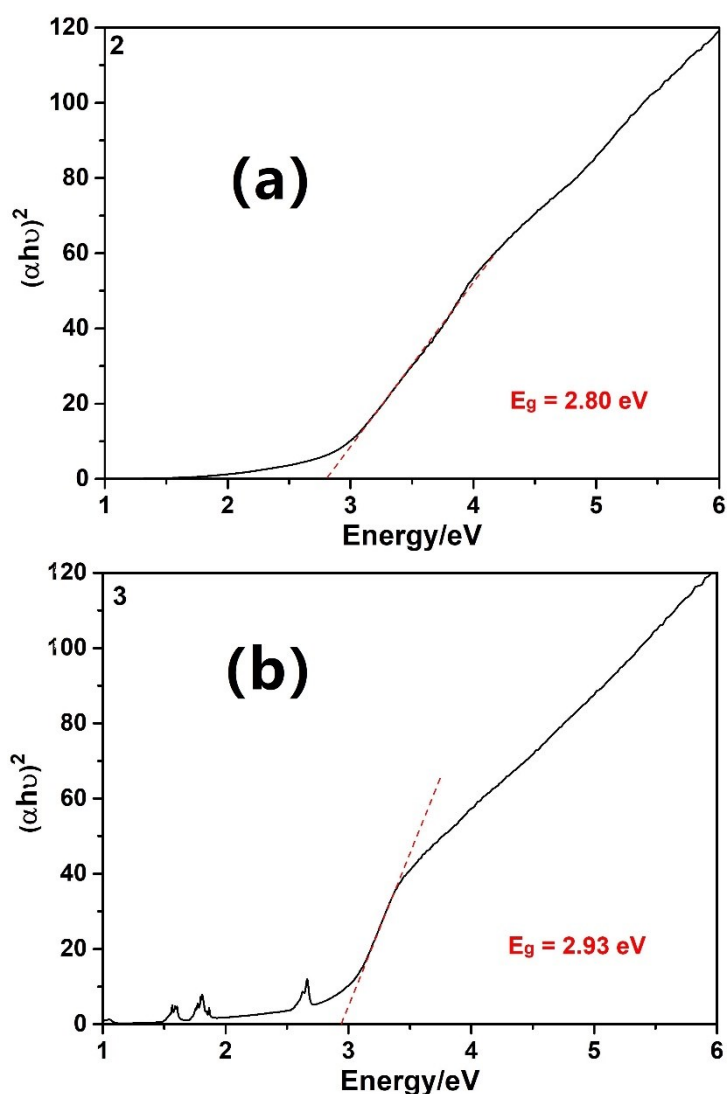


Fig. S4 UV-vis-NIR diffuse reflectance spectra for **2** (a) and **3** (b).

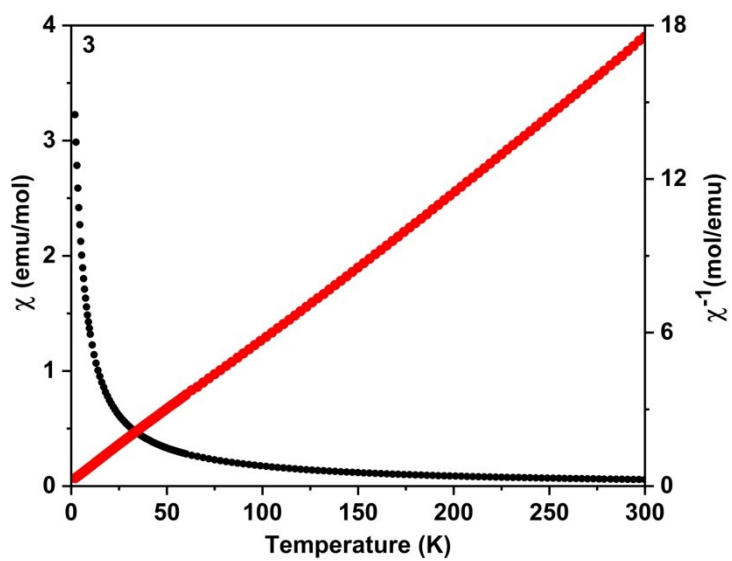
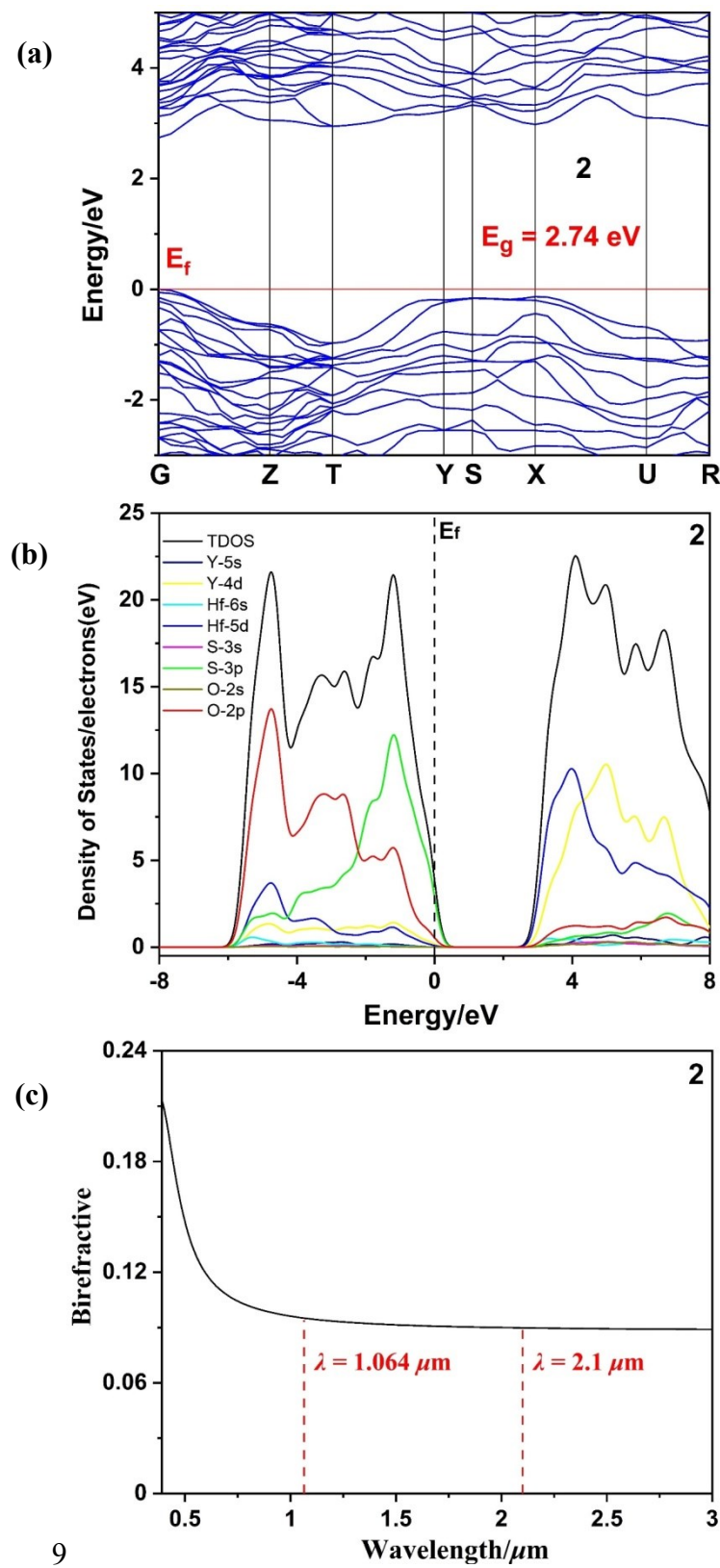


Fig. S5 Temperature-dependent magnetic susceptibility of 3.



9

Fig. S6 The calculated band structure (a), DOS (b), and birefringence (c) of **2**. Fermi level is set at 0 eV.

- 1 V. Tallapally, T. A. Nakagawara, D. O. Demchenko, Ü. Özgür, I. U. Arachchige, *Nanoscale* 2018, **10**, 20296–20305.
- 2 P. Makula, M. Pacia, W. Macyk, *J. Phys. Chem. Lett.* 2018, **9**, 6814–6817.
- 3 P. Kubelka, F. Munk, *Z. Technol. Phys.* 1931, **12**, 593–599.
- 4 S. J. Clark, M. D. Segall, C. J. Pickard, P. J. Hasnip, M. I. J. Probert, K. Refson, M. C. Payne, *Z. Kristallogr.* 2005, **220**, 567–570.
- 5 F. Bassani and G. P. Parravicini, *Electronic States and Optical Transitions in Solids*; Pergamon Press Ltd.: Oxford, U.K., 1976.
- 6 M. Gajdoš, K. Hummer, G. Kresse, J. Furthmüller and F. Bechstedt, *Phys. Rev. B*, 2006, **73**, 045112.
- 7 S. Laksari, A. Chahed, N. Abbouni, O. Benhelal and B. Abbar, *Comp. Mater. Sci.*, 2006, **38**, 223–230.
- 8 S. D. Mo and W. Y. Ching, *Phys. Rev. B*, 1995, **51**, 13023.
- 9 J. A. Cody, C. Deudon, L. Cario, A. Meerschaut, *Mater. Res. Bull.* 1997, **32**, 1181–1192.
- 10 C. Deudon, A. Meerschaut, L. Cario, J. Rouxel, *J. Solid State Chem.* 1995, **120**, 164–169.
- 11 J. A. Cody, J. A. Ibers, *J. Solid State Chem.* 1995, **114**, 406–412.
- 12 L. Cario, C. Deudon, A. Meerschaut, J. Rouxel, *J. Solid State Chem.* 1998, **136**, 46–50.
- 13 C. Boyer-Candalen, C. Deudon, A. Meerschaut, *J. Solid State Chem.* 2000, **152**, 554–559.
- 14 C. Boyer-Candalen, J. Derouet, P. Porcher, Y. Moëlo, A. Meerschaut, *J. Solid State Chem.* 2002, **165**, 228–237.
- 15 A. S. Gardberg, J. A. Ibers, *Z. Kristallogr.* 2001, **216**, 491–492.